https://doi.org/10.5194/bg-2019-478
Preprint. Discussion started: 16 January 2020


Biogeosciences Discussions
Open Access
EGU

# Linking climatic-driven iron toxicity and water stress to a massive mangrove dieback

James Z. Sippo[1,2], Isaac R. Santos[2,3], Christian J. Sanders[2], Patricia Gadd[4], Quan Hua[4], Catherine Lovelock[5], Nadia S. Santini[6,7], Scott G. Johnston[1], Yota Harada[8], Gloria Reithmeir[1], Damien T. Maher[1,9]

[1]Southern Cross Geoscience, Southern Cross University, Lismore, 2480 Australia.
[2]National Marine Science Centre, Southern Cross University, PO Box 4321, Coffs Harbour, NSW 2450, Australia
[3]Department of Marine Sciences, University of Gothenburg, Sweden
[4]Australian Nuclear Science and Technology Organisation (ANSTO), Locked Bag 2001, Kirrawee DC, NSW 2232, Australia
[5]School of Biological Sciences, the University of Queensland, St Lucia QLD 4072, Australia
[6]Cátedra Consejo Nacional de Ciencia y Tecnología, Av. Insurgentes Sur 1582, Crédito Constructor, Benito Juárez, 03940, Ciudad de México, Mexico.
[7]Instituto de Ecología, Universidad Nacional Autónoma de México, Ciudad Universitaria, 04500, Ciudad de México, Mexico.
[8]Australian Rivers Institute – Coast and Estuaries, and School of Environment and Science, Griffith University, Gold Coast, QLD 4222, Australia
[9]School of Environment, Science and Engineering, Southern Cross University, Lismore 2480, Australia

## Abstract

*A massive mangrove dieback event occurred in 2015/2016 along ~1000km of pristine coastline in the Gulf of Carpentaria, Australia. To gain insights into dieback drivers, we combine sediment and wood chronologies to analyze geochemical and climatic changes. The unique combination of low rainfall and low sea level observed during the dieback event was unprecedented in the previous three decades. Multiple lines of evidence from iron (Fe) chronologies in wood and sediment, wood densities and mangrove water use efficiency suggest low water availability within the dead mangrove forest. Wood and sediment chronologies suggest a rapid and large mobilization of sedimentary Fe, which was likely associated with pyrite oxidation within mangrove sediments. High resolution elemental analysis of wood cross sections revealed 30-90 fold increase in Fe concentrations in dead mangrove areas just prior to mortality. Fe concentrations in wood samples correlated strongly with the El Niño Southern Oscillation (ENSO) index, suggesting ENSO was a major driver of Fe mobilization. Large Fe losses from sediments during the dieback are consistent with Fe uptake in the trees, further implying sediment pyrite oxidation. If our data are representative of the entire dieback region, we estimate that the dieback drove the mobilization and loss of 50 ± 173 Gg Fe, equivalent to 8-50% of annual global atmospheric Fe deposition into the oceans, which is one of the major drivers of surface ocean productivity. Overall, our observations support the hypothesis that the forest dieback was associated with low water availability and Fe toxicity driven by a strong ENSO event.*

https://doi.org/10.5194/bg-2019-478
Preprint. Discussion started: 16 January 2020




## Introduction

Mangroves provide a wide range of ecosystem services such as nursery habitat, carbon sequestration, and coastal protection (Barbier et al. 2011, Donato et al. 2011). Climate change is a major threat to mangroves adding to the threats imposed by deforestation and over exploitation (Hamilton and Casey 2016, Richards and Friess 2016). Rising sea levels, changing sediment budgets, reduced water availability and increasing climatic extremes are negatively affecting mangroves (Gilman et al. 2008, Alongi 2015, Lovelock et al. 2015, Sippo et al. 2018). In Australia, an extensive mangrove dieback event occurred in the Gulf of Carpentaria, in December 2015 - January 2016, coincident with extreme drought and low sea level. This extreme climatic event drove the largest recorded mangrove mortality event (~1000 km coastline, ~7400 ha) driven by natural causes (Duke et al., 2017; Harris et al., 2017; Sippo et al., 2018). Two other large scale mangrove dieback events occurred at the same time in Australia. One was reported in Exmouth, Western Australia (Lovelock et al. 2017) and another occurred in Kakadu National Park, Northern Territory, Australia (Asbridge et al. 2019).

The mangrove mortality has been attributed to low water availability associated with extreme drought. The limited rainfall and groundwater availability, and anomalously low sea level reduced tidal inundation and soil water content (Duke et al., 2017; Harris et al., 2017). A strong El Niño event resulted in the lowest recorded rainfall in the nine months preceding the mangrove dieback since 1971, and regional sea levels that were 20 cm lower than normal (Harris et al., 2017). Atmospheric moisture was also unusually low during 2015, which may influence the physiological functioning of mangrove trees (Nguyen et al. 2017). The climatic and hydrologic changes may affect both plant physiology and sediment geochemistry. Here, we explore whether low sediment water content and associated changes in sediment geochemistry may have played a role in the dieback.

In contrast to terrestrial forest soils, mangrove sediments are largely anoxic due to their water-logged nature, and high organic matter contents. Mangrove sediments also receive a supply of materials from both terrestrial environments (e.g. Fe, sediments) and oceanic water (e.g. $SO_4$) which results in distinctly different biogeochemical cycling within the sediments than terrestrial forests (Burdige 2011). As a result, mangrove sediments often accumulate bioauthigenic pyrite ($FeS_2$) which remains stable under reducing conditions (van Breemen 1988, Johnston et al. 2011). Lowering of water levels can alter sediment redox conditions and result in the oxidation of $FeS_2$, releasing acid and dissolved Fe (mostly as $Fe^{2+}$) to porewater (Burton et al. 2006, Johnston et al. 2011, Keene et al. 2014). Subsequent oxidation of $Fe^{2+}$ and precipitation of $Fe^{3+}$ (oxy)hydroxide minerals can then lead to the accumulation of highly reactive Fe in sediments. Reactive $Fe^{3+}$ minerals are in turn readily subject to reductive dissolution and (re)-formation of $Fe^{2+}$ during any switches to reducing conditions. Thus, changes in sediment redox conditions, i.e. increased oxidation and consequent reduction, in mangrove sediments that are rich in $FeS_2$ can cause a release of bioavailable $Fe^{2+}$.

Mangrove uptake of $Fe^{2+}$ may be a powerful proxy of historic sediment redox conditions, driven by short and long-term variability in sea-level. High levels of bioavailable Fe may also be associated with tree mortalities, although there is limited evidence of Fe toxicity. Fe toxicity in some mangrove species can occur at concentrations ~2 fold higher than the optimal Fe supply for maximal growth (Alongi, 2010). Since Fe is often a limiting nutrient in

https://doi.org/10.5194/bg-2019-478
Preprint. Discussion started: 16 January 2020




ocean surface water, Fe outwelling from mangroves could have important implications for productivity in coastal waters (Jickells and Spokes , Fung et al. 2000, Holloway et al. 2016).

An extensive saltmarsh dieback in southern United States in 2000 provides an analogue to the mangrove dieback studied here. The saltmarsh dieback coincided with drought conditions (McKee et al. 2004, Ogburn and Alber 2006, Alber et al. 2008). McKee et al. (2004) found that sediments in dead saltmarsh areas had significantly higher acidification upon oxidation than alive areas. The dieback may have been caused by reduced water availability, increased sediment salinities and/or metal toxicity associated with soil acidification following sediment pyrite oxidation. However, the cause of the dieback was debated and remains inconclusive (McKee et al. 2004, Silliman et al. 2005, Alber et al. 2008). In contrast to the herbaceous salt marsh species in the US dieback, mangroves are woody, providing opportunities for climatic reconstructions (Verheyden et al. 2005, Brookhouse 2006). To date, the use of dendrochronological techniques have not been used to assess changes in sediment geochemistry in mangroves.

Here, we combine multiple wood and sediment chronology techniques to reconstruct sediment geochemistry and assess links to climate. To evaluate the potential for mobilisation of Fe during the dieback, we combine multiple lines of evidence including: 1) micro X-ray fluorescence (Itrax) to analyse the elemental composition in wood and sediment cores; 2) wood density measurements, tree growth rates and $\delta^{13}C$ isotopes to assess historic changes in water availability (Santini et al. 2012, Santini et al. 2013, Van Der Sleen et al. 2015, Maxwell et al. 2018); and 3) sediment profiles of $FeS_2$ concentrations to give insight into sediment redox conditions and Fe mobilisation. We assess these parameters in areas where mangroves died and where they survived the dieback event.

## Methods

### Study Site

This study was conducted in the South Eastern corner of the Gulf of Carpentaria, in Northern Australia (Figure 1). The Gulf of Carpentaria is a large and shallow (< 70 m) waterbody with an annual rainfall of 900mm per year and a semi-arid climate (Bureau of Meteorology; Duke et al., 2017). The region has low lying topography with abundant mangroves and extensive saltpans in the upper intertidal zone (Duke et al., 2017). The species *Avicennia marina* and *Rhizophora stylosa* dominate the mangroves within the Gulf of Carpentaria.

Widespread dieback of the mangroves in the region was observed in 2015-2016. The dieback predominantly affected *A. marina* which occupy the open coastlines and upper intertidal areas (Duke et al., 2017). Although 7500 ha of mangrove suffered mortality some areas remained relatively unaffected, providing an opportunity to compare conditions in live and dead stands. We assessed a live and dead mangrove area 20 months after the dieback event. The two mangrove areas were separated by the Norman River and were ~ 4 km apart (Figure 1). The living mangrove has an area of 175 ha and had some dead trees in the upper intertidal zone and living trees that showed signs of stress (dead branches and partial defoliation). Towards the seaward edge, the forest had no signs of canopy loss 8 months post dieback event. The dead mangrove area was 169 ha and had close to 100% mortality (Figure 1b), with only some trees at the waterline showing regrowth.

https://doi.org/10.5194/bg-2019-478
Preprint. Discussion started: 16 January 2020


Biogeosciences
Discussions
Open Access
EGU

**Figure 1. Study sites of a) living mangrove area (green) and b) dead mangrove area (red) near to the mouth of the Norman River, Karumba Qld. Note: The yellow 'x' symbols represent transects through the upper, middle and lower study sites. c) Elevation above the Australian Height Datum (AHD) from Lidar DEM were measured from the seaward mangrove edge in 2017 from the same transects as samples were collected in 2016 through the living (Green line) and dead (red line) mangrove area (data available from http://wiki.auscover.net.au/wiki/Mangroves). Satellite images sourced from © Google Earth (2019) and Queensland Government (2019).**

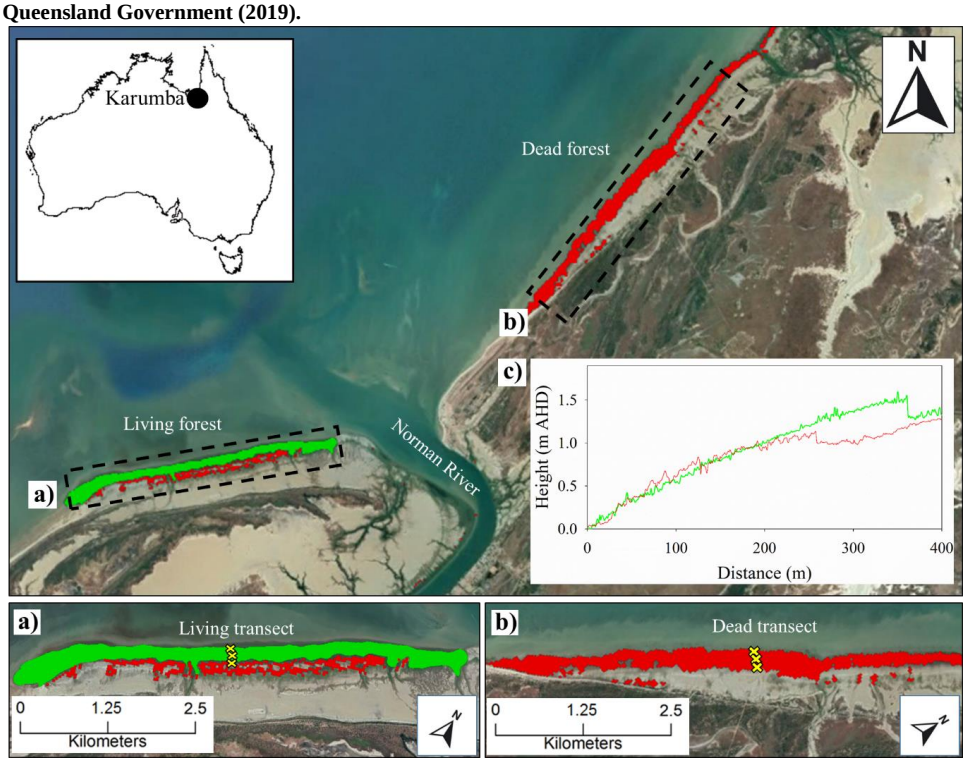


## Field sampling and chemical and isotopic analyses

Tree and sediment samples were collected in August 2017 approximately 20 months after the dieback event. Wood and sediment samples were collected from transects from the lower intertidal zone to the upper intertidal zone (Figure 1). Fully mature trees were selected at ~20 m inward from the lower and upper intertidal forest edges and in the centre of the forest. One upper, mid and lower tide wood sample was taken in living and dead mangrove areas (Figure 1a and b). Wood samples from *A. marina* were taken from 50 cm above ground level by cutting a 1cm thick disk from the trunk. At the upper and lower intertidal sites, two sediment cores were taken. One core, taken to 2 m with a Russian peat auger with extensions, was sampled for elemental analysis with Itrax. A second core, taken to a depth of 1 m using a tapered auger corer in August 2018 at the same site, was sampled for analysis of chromium reducible sulfur (CRS).

Wood samples were dated using bomb $^{14}C$ (eg, Santini et al. 2013; Witt et al. 2017). Water-use efficiency (WUE), which is the ratio of net photosynthesis to transpiration, was assessed using wood cellulose stable isotopic composition $\delta^{13}C$ following (Van Der Sleen et al. 2015)

https://doi.org/10.5194/bg-2019-478
Preprint. Discussion started: 16 January 2020




as water use efficiency correlates with larger values of $\delta^{13}C$ (Farquhar and Richards 1984, Farquhar et al. 1989). Wood elemental composition and density was assessed using micro X-ray fluorescence. Sub-samples for $^{14}C$ and $\delta^{13}C$ were taken along the longest radius of each wood disk at regular intervals from the centre of the wood disc to the outer edge (youngest wood). The sub-samples were collected using a scalpel parallel to tree rings to reduce errors. Alpha cellulose was extracted from the wooden sub-samples (Hua et al. (2004b), combusted to $CO_2$ and converted to graphite (Hua et al. 2001). A portion of graphite was used for the determination of $\delta^{13}C$ for isotopic fractionation correction using a Micromass IsoPrime elemental analyser/isotope ratio mass spectrometer (EA/IRMS) at the Australian Nuclear Science and Technology Organisation (ANSTO). The remaining graphite was analysed for $^{14}C$ using the STAR accelerator mass spectrometry (AMS) facility at ANSTO (Fink et al. 2004) with a typical analytical precision of better than 0.3% (2σ).

Wood samples and sediment cores were analysed for elemental composition with a micro X-ray fluorescence conducted at ANSTO using an Itrax core scanner (Cox Analytical Systems). The scanner produces a high resolution (0.2 mm) radiographic density pattern and semi-quantitative elemental profiles for each sample. The Itrax measured 34 elements, but we only report Fe. Wood samples were scanned along the same transect as for $^{14}C$ samples, i.e. the longest radius from the wood core to the outer edge. Sediment cores were analysed using the Itrax in four 50 cm increments. Chromium reducible sulfur (CRS) was measured from sediment samples collected with a Russian peat auger to 1 m depth to provide an estimate of reducible inorganic S (RIS; Burton et al. (2008). CRS subsamples were placed in bags with air removed and frozen prior to CRS analysis. Groundwater salinity values were taken at the same sites as wood samples from bore holes dug to ~1m depth. Groundwater in the holes was purged and allowed to refill and salinities were measured using a Hach multi-sonde.

**Data analysis**

Radiocarbon values were used to calculate calendar ages. To align dates with Itrax data, we interpolated ages using the wood circumference. Itrax elemental and density data were normalized as the mean subtracted from each value divided by the standard deviation following the calculation of Z-scores by Hevia et al. (2018) and are referred to hereforth as relative concentrations. This normalization allows a more direct comparison between samples from living and dead areas. Growth rates in mm per year were calculated as the measured increment divided by the difference in years (calculated from $^{14}C$) between samples. De-trended growth rates were then calculated as the deviation from the exponential curve fitted to growth rates for each sample. Water use efficiency (WUE) was calculated from $\delta^{13}C$ isotope values (Van Der Sleen et al. 2015). Differences in WUE between living and dead mangrove areas were compared using T-test.

Cross correlations with a time lag of one-month intervals were used to evaluate the relationships between climatic variables (the Southern Oscillation Index (SOI), sea level, rainfall and vapour pressure) with wood density, elemental relative concentrations and growth rates. SOI data and other climate data were obtained from the Bureau of Meteorology (Station number 029028, 2019) and published reports (Jones et al. 2009, Harris et al. 2017). All climatic data were used with a one month resolution and were standardised using a centred moving mean.

**Results**

**Climatic conditions**

https://doi.org/10.5194/bg-2019-478
Preprint. Discussion started: 16 January 2020


Biogeosciences
Discussions
Open Access
EGU

The climate records over the last three decades reveal an unprecedented combination of low sea level and low annual rainfall. SOI is significantly correlated to all climate variables (Pearson product moment correlation, $P < 0.05$). Lower sea levels and rainfall had previously occurred independently (Figure 2). Since 1985, trends in SOI index based on vapour pressure, precipitation and sea level observations show El Niño in 1983, 1987, 1992, 1994, 1998, 2015 and 2016.

**Figure 2. Centred moving means of climate data from the South Eastern Gulf of Carpentaria Australian (Jones et al. 2009, Harris et al. 2017, Bureau of Meteorology 2019). The grey bar represents the period during which the dieback event occurred.**

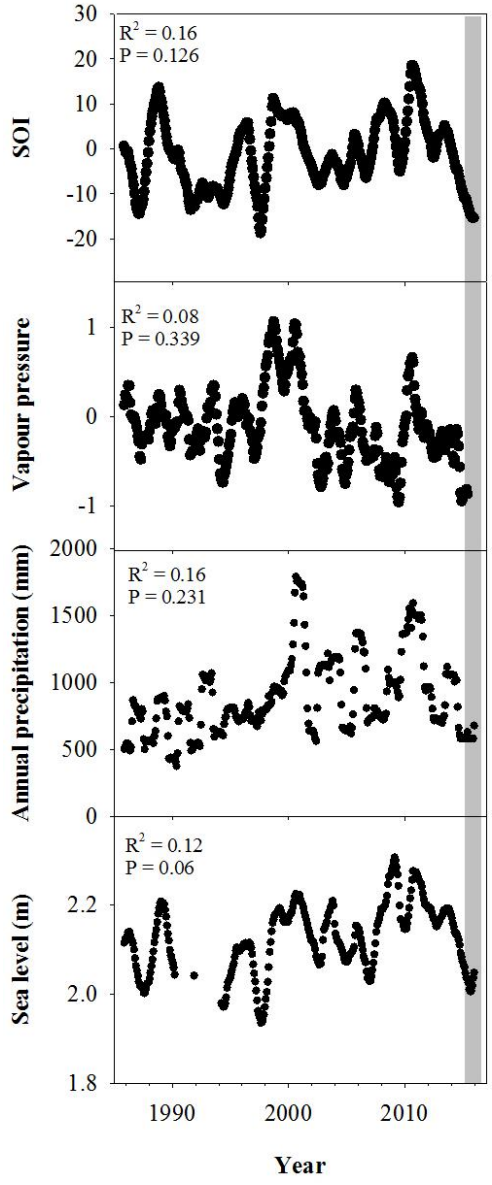

https://doi.org/10.5194/bg-2019-478
Preprint. Discussion started: 16 January 2020




**Wood samples and ages** –The ages of *A. marina* ranged from 15 ± 2 to 34 ± 2 years (Table 1). On average, the trees in the living and dead mangrove forests were 21 ± 4 and 34 ± 1 years old respectively. Tree growth rates that were de-trended to negative exponential growth had no trends over time in either the living or dead mangrove areas (Table 1).

**Table 1. Summary of radiocarbon ages and growth rates (deviation from exponential growth) for all wood samples taken from dead and living mangrove areas in the Gulf of Carpentaria, Australia.**

| Sample | Distance from pith (mm) | $^{14}$C Mean ±2σ (pMC) ** | | | Modelled calendar age Mean ±1s (year AD) | | | Deviation from negative exponential growth (mm per year) |
|---|---|---|---|---|---|---|---|---|
| **Dead mangrove** | | | | | | | | |
| **Upper intertidal** | 2 | 122 | ± | 0.3 | 1984 | ± | 2 | - |
| | 17 | 119.8 | ± | 0.3 | 1986 | ± | 2 | -2.6 |
| | 35 | 118 | ± | 0.3 | 1988 | ± | 2 | -1.4 |
| | 52 | 116.1 | ± | 0.3 | 1990 | ± | 3 | -1.2 |
| | 70 | 110.9 | ± | 0.3 | 1998 | ± | 2 | -4.7 |
| | 87 | 105.4 | ± | 0.2 | 2010 | ± | 2 | -1.3 |
| | 89 | | | | 2015* | | | -0.9 |
| **Mid intertidal** | 2 | 123.6 | ± | 0.3 | 1983 | ± | 2 | - |
| | 12 | 122.8 | ± | 0.3 | 1984 | ± | 2 | 2.3 |
| | 24 | 119.1 | ± | 0.3 | 1987 | ± | 2 | -4.8 |
| | 36 | 115.9 | ± | 0.4 | 1991 | ± | 3 | -3.6 |
| | 49 | 110.1 | ± | 0.3 | 1999 | ± | 2 | -3.7 |
| | 62 | 105.2 | ± | 0.3 | 2011 | ± | 3 | -0.2 |
| | 64 | | | | 2015* | | | -0.2 |
| **Lower intertidal** | 2 | 123.3 | ± | 0.4 | 1983 | ± | 2 | - |
| | 23 | 120.4 | ± | 0.4 | 1986 | ± | 2 | -2.3 |
| | 45 | 117.4 | ± | 0.4 | 1989 | ± | 2 | -1.8 |
| | 89 | 110.9 | ± | 0.3 | 1998 | ± | 2 | -1.9 |
| | 110 | 105.8 | ± | 0.3 | 2009 | ± | 2 | -2.1 |
| | 113 | | | | 2015* | | | -2.5 |
| **Living mangrove** | | | | | | | | |
| **Upper intertidal** | 2 | 163.8 | ± | 0.5 | 1995 | ± | 2 | - |
| | 20 | 112 | ± | 0.4 | 1996 | ± | 3 | 2.3 |
| | 40 | 109.8 | ± | 0.4 | 2000 | ± | 3 | -0.8 |
| | 58 | 103.7 | ± | 0.4 | 2013 | ± | 2 | -2.3 |
| | 60 | | | | 2017* | | | -2.9 |
| **Mid intertidal** | 2 | 113.3 | ± | 0.5 | 1994 | ± | 2 | - |
| | 16 | 111.1 | ± | 0.3 | 1997 | ± | 2 | -1.0 |
| | 33 | 109.2 | ± | 0.4 | 2001 | ± | 2 | 0.8 |
| | 49 | 106.6 | ± | 0.3 | 2014 | ± | 2 | -1.2 |
| | 50 | | | | 2017* | | | -2.3 |

https://doi.org/10.5194/bg-2019-478
Preprint. Discussion started: 16 January 2020




| | | | | | | | | |
|---|---|---|---|---|---|---|---|---|
| **Mid intertidal** | 2 | 113.4 | ± | 0.3 | 1993 | ± | 3 | - |
| | 25 | 110.9 | ± | 0.3 | 1998 | ± | 2 | -1.0 |
| | 50 | 101.9 | ± | 0.3 | 2017 | ± | 1 | 0.2 |
| | 51 | | | | 2017* | | | -2.3 |
| **Lower intertidal** | 2 | 108.8 | ± | 0.3 | 2002 | ± | 2 | - |
| | 17 | 107.3 | ± | 0.3 | 2005 | ± | 2 | -5.1 |
| | 33 | 104.9 | ± | 0.4 | 2011 | ± | 3 | 9.2 |
| | 46 | 104.3 | ± | 0.3 | 2014 | ± | 2 | -2.3 |
| | 48 | | | | 2017* | | | -2.2 |

* Date of collection of *A. marina* samples
**Measured $^{14}C$ content is shown in percent Modern Carbon (pMC; Stuiver and Polach 1977)

**Fe in wood and sediment cores -** Fe relative concentrations in all dead mangrove samples peaked at the time of mangrove mortality in late 2015/early 2016 (Figure 3). In the living mangrove samples, Fe peaked in late 2015/early 2016 and then decreased in 2016 and 2017 back to average levels. Peak Fe concentrations in the upper, mid and lower intertidal areas of the dead mangrove samples were 40, 90 and 30 fold higher than their mean baseline concentrations, respectively. In the living mangrove area, peak Fe concentrations in the upper, mid and lower intertidal areas were 25, 4 and 3 fold higher than their mean baseline concentrations, respectively. In the dead mangrove area, Fe levels were similar from the upper to the lower intertidal zone (Figure 3). In the living mangrove area, Fe was highest in the upper and mid intertidal zone and decreased in the lower intertidal zone.

https://doi.org/10.5194/bg-2019-478
Preprint. Discussion started: 16 January 2020




**Figure 3. Fe relative concentrations in mangrove wood over time in living (green dots) and dead (red dots) from upper, mid and lower intertidal areas of mangroves of the Gulf of Carpentaria, Australia. Grey areas indicate the dieback event.**

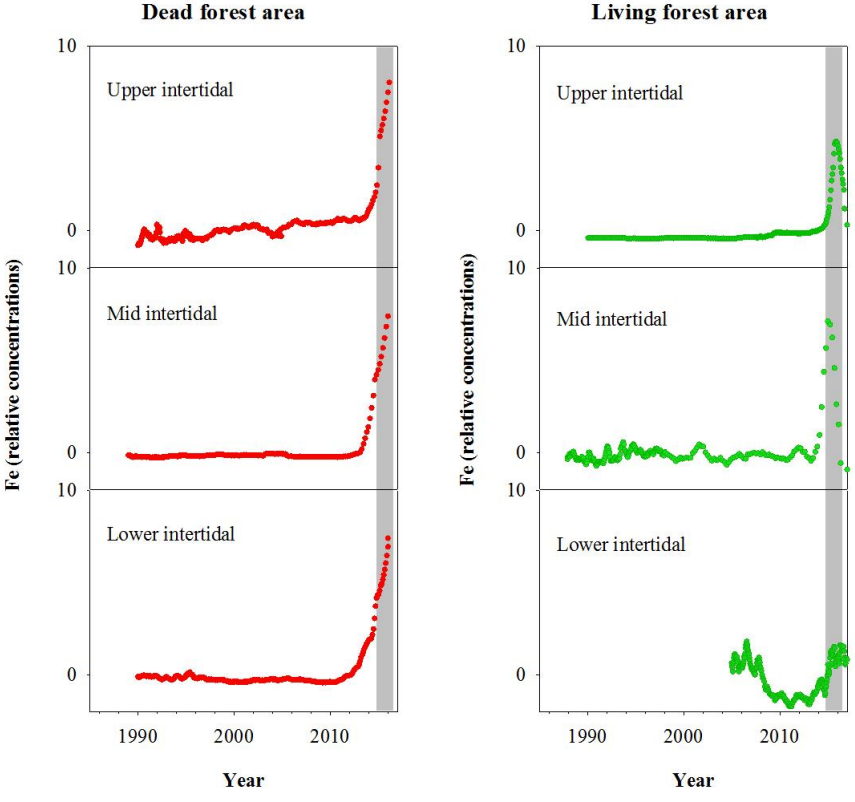


Significant correlations with no time lag were found between Fe in wood and vapour pressure, rainfall, sea level and SOI (Figure 4). All climate variables were strongly correlated with SOI. Therefore, we could not separate the influence of individual climate variables on wood Fe. In the dead and living mangrove areas, the strongest correlations with Fe occurred with no time lag (Figure 4).

https://doi.org/10.5194/bg-2019-478
Preprint. Discussion started: 16 January 2020




**Figure 4. Cross correlation function (CCF) between Fe in wood samples and climate data at one month resolution over a 12 month period prior and post dieback. Wood samples are from the upper, mid and lower intertidal zones of the dead (red) and living (green) mangrove areas. Blue horizontal dashed lines indicate P< 0.01 with n=125. Grey dashed vertical lines at zero lag indicate dieback period and the grey bar represents the period during which the dieback event occurred.**

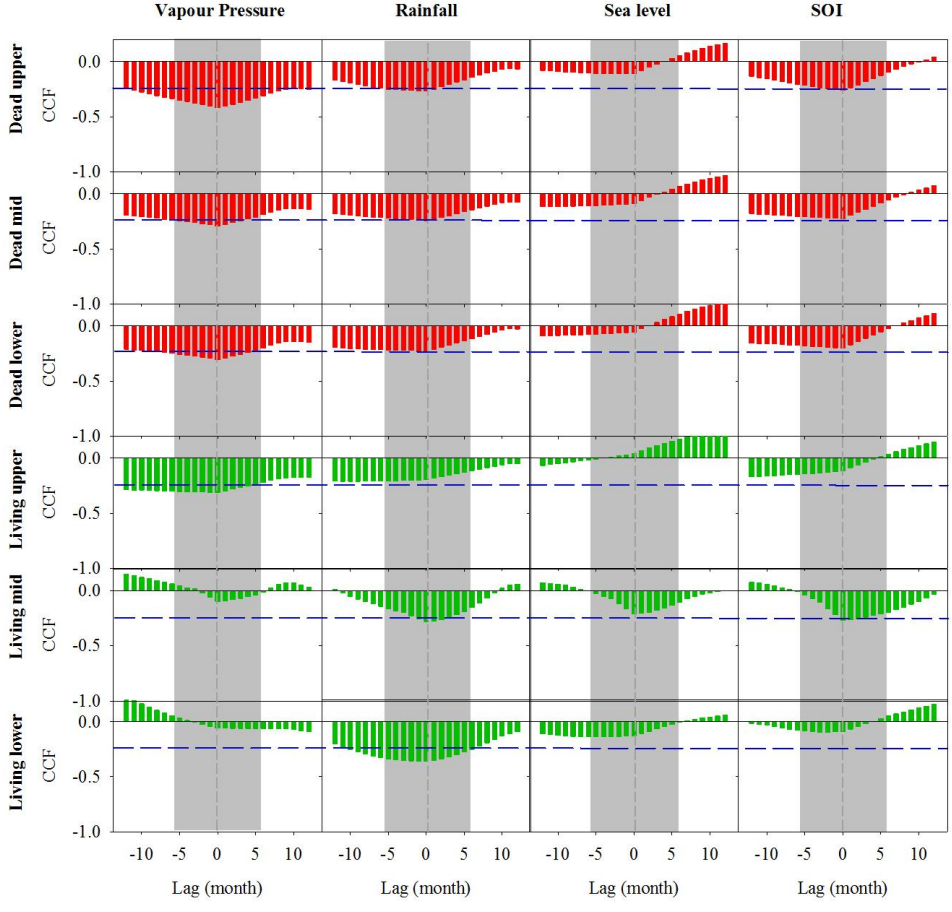


Sediment cores had a similar pattern of decreasing Fe with depth in upper and lower intertidal areas, and in living and dead mangrove areas (Figure 5a). Dead mangrove areas were depleted with Fe by ~32% in the surface 50 cm and ~26% in the surface 1 m relative to the respective living mangrove areas in both the upper and lower intertidal area (Figure 5b, c and d). Fe relative concentrations were significantly higher in living mangrove areas compared to dead mangrove areas (Mann-Whitney Rank Sum Test, $P < 0.001$ for all depths).

https://doi.org/10.5194/bg-2019-478
Preprint. Discussion started: 16 January 2020


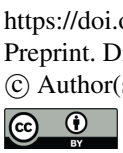

Biogeosciences
Discussions
Open Access
EGU

**Figure 5. a) Fe relative concentrations in sediment cores to 2m depth from the upper and lower intertidal areas of living (green) and dead (red) mangroves in the Gulf of Carpentaria. b) Box plots of normalised Fe relative concentrations from sediment cores to b) 0.5 m, c) 1 m and d) 2 m depth. The central horizontal line represents the median value, the box represents the upper and lower quartiles, and the whiskers represent the maximum and minimum values excluding outliers, i.e., black dots.**

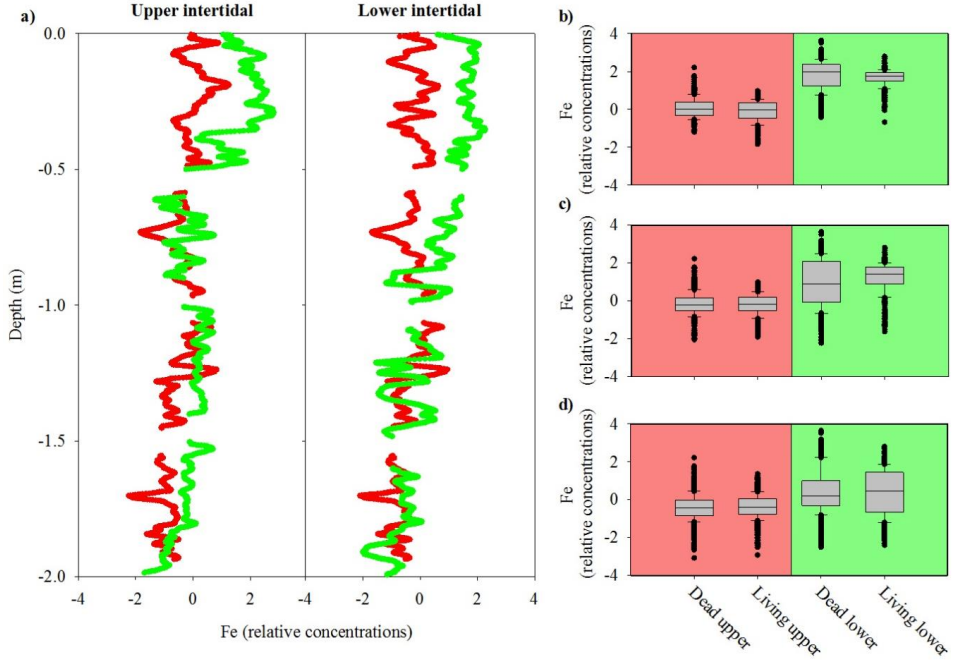


Chromium Reduced Sulfur (CRS) concentrations in sediment cores were lower in the dead than the living mangrove area by 36% in the upper and 38% in the lower intertidal zones. These differences were not significant (Mann-Whitney Rank Sum Test, $P > 0.05$) but were very similar to Itrax differences (Figure 6). Dead mangrove sediment CRS concentrations increased from ~10 cm depth. Living mangrove CRS increased from ~30 cm depth compared to lower levels deeper in the soil profile, implying some recent CRS loss. In the lower intertidal zone, CRS concentrations were highest from ~10 cm below the surface in both dead and living sediment samples and then decreased with depth.

https://doi.org/10.5194/bg-2019-478
Preprint. Discussion started: 16 January 2020




277 **Figure 6. Chromium reducible sulfur (CRS) profiles from sediment cores in dead (red) and living (green)**
278 **mangrove areas in the Gulf of Carpentaria.**

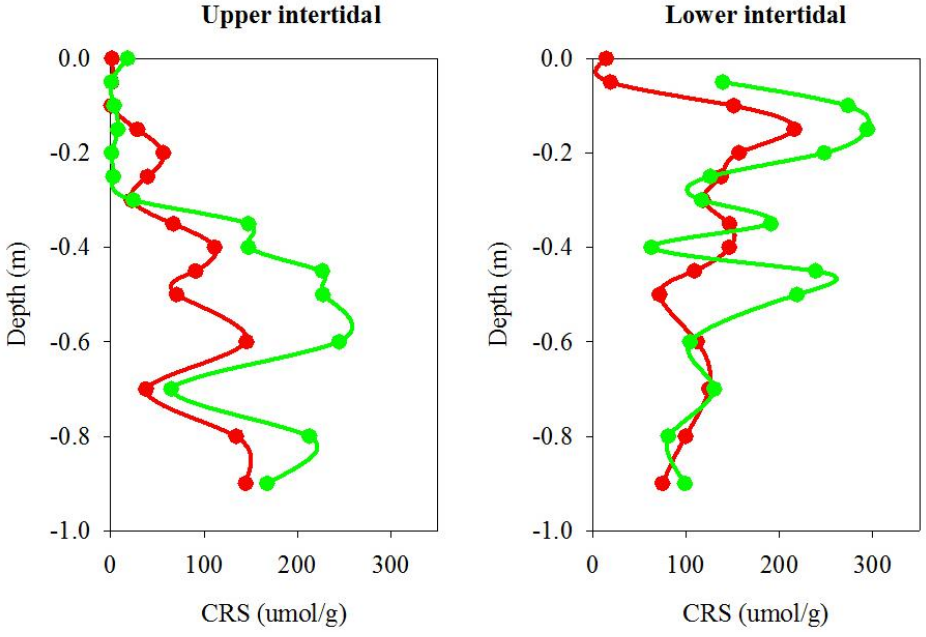


279

280 Water use efficiency (WUE) calculated from $\delta^{13}C$ decreased in all wood samples from 1983
281 to 2017 (Figure 7a), suggesting increasing water availability in the Gulf of Carpentaria.
282 During the dieback event, median WUE values were higher in dead samples than in living
283 samples, with the differences more pronounced in the upper intertidal zones (Figure 7b).
284 Comparison of WUE in dead and living mangrove samples suggests lower water availability
285 in the dead mangrove area (Figure 7b). However, the mean WUE values were compared from
286 1983 to 2017 and were not significantly different (T-test, P = 0.2) in dead and living
287 mangrove areas. Groundwater salinity values were highest in the upper intertidal mangrove
288 areas and lowest in the lower intertidal areas (Figure 7c). Salinities were not significantly
289 different in the living and dead forest areas (T-test, P = 0.913).

290

https://doi.org/10.5194/bg-2019-478
Preprint. Discussion started: 16 January 2020


Biogeosciences
Discussions
Open Access
EGU

**Figure 7. a) Changes to Water Use Efficiency (WUE) over time in wood samples collected from the upper, lower and mid intertidal zone in living (green) and dead (red) mangrove areas. The grey bar represents the mangrove dieback event. Error bars represent standard error but are not visible due to low error of individual samples. b) Box plot of water use efficiency in mangrove wood samples in dead and living mangrove areas in the upper, mid and lower intertidal zones. Sample size > 4 from each wood sample. The central horizontal line represents the median, the box represents the upper and lower quartiles, and the whiskers represent the maximum and minimum values. c) Box plot of groundwater salinity eight months post dieback event in dead and living mangrove areas in the upper, mid and lower intertidal zones. Sample size > 3 from each intertidal zone.**

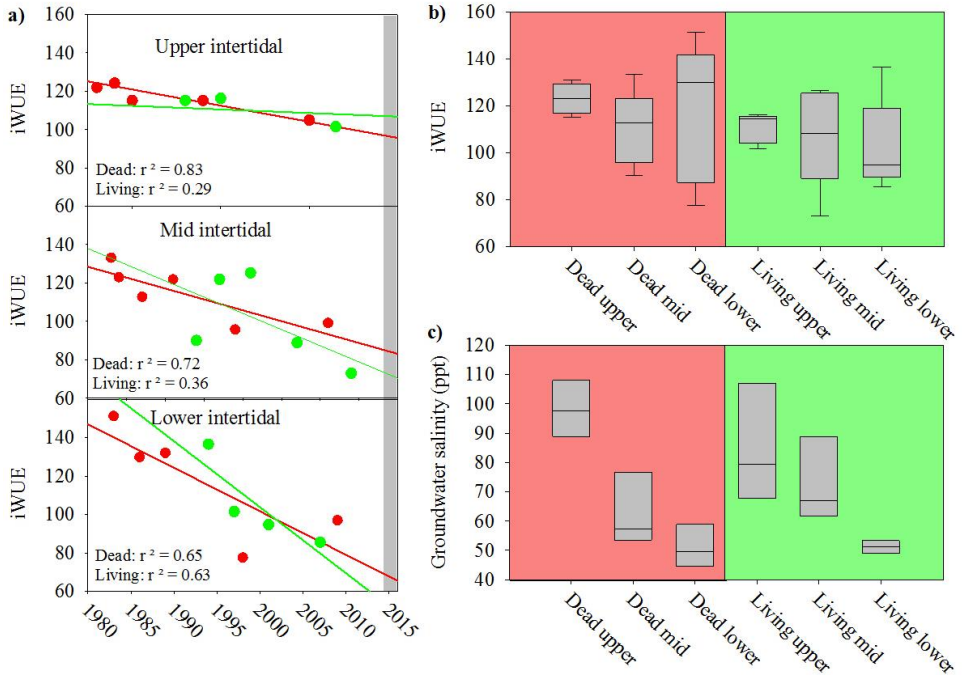

https://doi.org/10.5194/bg-2019-478
Preprint. Discussion started: 16 January 2020




Normalised wood density values in the dead mangrove forest showed no change during the dieback event in the upper intertidal zone, but a decline in density values occurred in the mid and lower intertidal zones (Figure 8). In the living mangrove area, declines in wood density values occurred in the upper and mid intertidal zones during the mortality event, but no variation in density occurred in the lower intertidal zone (Figure 8).

**Figure 8. Normalised wood density (relative concentrations) in mangrove wood over time in living (green dots) and dead (red dots) mangrove areas of the Gulf of Carpentaria, Australia. The grey bar represents the time period of the dieback event.**

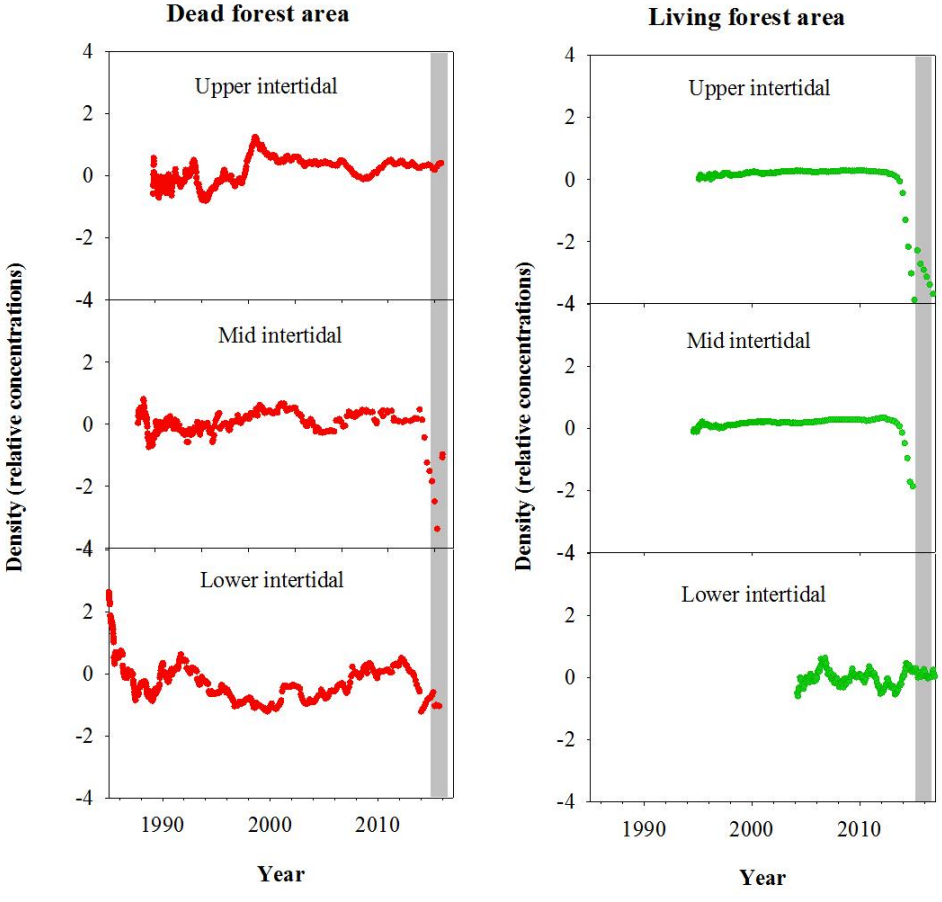

https://doi.org/10.5194/bg-2019-478
Preprint. Discussion started: 16 January 2020




311 **Discussion**

312 **Evidence of changes in water availability from dendrogeochemistry**

313 Multiple lines of evidence from wood samples and sediment cores demonstrated differences
314 in water availability between the dead and living mangrove areas. Most importantly, Fe
315 trends in wood and sediment samples suggest the mobilisation of bioavailable Fe as $Fe^{2+}$
316 when bioauthigenic pyrite is oxidised and is also remobilised during the reduction of $Fe^{3+}$ if
317 conditions return to anaerobic (Johnson et al. 2011). The most likely cause for a shift from
318 reducing to oxidising conditions in the sediment is a reduction in water content (Keene et al.
319 2014) associated with the intense El Niño of 2015/16 and associated low sea level and annual
320 rainfall (Figure 2). Trends in wood density, mangrove growth rate and water use efficiency
321 also reveal distinct differences in water availability between dead and living forest areas.

322 **Fe in wood -** Elemental composition from wood samples provide strong evidence that the
323 mangrove forest experienced sharp changes in sediment geochemistry during the dieback
324 phase (Figure 3). This is consistent with low sea level and low rainfall/groundwater reducing
325 soil water content, leading to oxidation of Fe sulphide minerals and release of $Fe^{2+}$. The Fe
326 peak in the dead mangrove area at the time of tree mortality were 30 to 90 fold higher than
327 baseline Fe (the mean Fe concentration in the sample prior to the dieback event). In the living
328 mangrove area, an Fe peak 25 fold higher than baseline Fe was observed in the upper
329 intertidal zone (Figure 1). In the mid and lower intertidal areas of the living mangroves, Fe
330 peaks were 4 and 3 fold higher than baseline respectively. In all living wood samples, Fe
331 decreased after the dieback event, which suggests that Fe in new wood growth was reduced in
332 associated with a return to reducing sediment conditions and a concomitant reduction in $Fe^{2+}$
333 availability.

334 Records of all climate variables are in resolution of months, but the chronology of Fe (based
335 on $^{14}C$ dates) is in years. We therefore used time lag analysis to examine relationships
336 between climate variables and Fe over a two year period (Figure 4). Fe wood concentrations
337 over time were significantly correlated with rainfall and vapour pressure in the dead and
338 living forest areas (Figure 4). However, because all climate variables were strongly correlated
339 to each other, we were unable to separate the relationships between individual climate drivers
340 and Fe trends. We anticipate that the combination of low availability of fresh groundwater
341 and low sea level associated with the strong El Niño event of 2015/16 are drivers of the
342 sediment redox conditions which are reflected in wood Fe trends.

343 Considering the extreme increases in Fe concentrations observed in the wood samples
344 coinciding with the dieback event, Fe toxicity could have caused mangrove mortality. Alongi,
345 (2010) found that Fe toxicity occurred in some mangrove species at high concentrations
346 (100mmol $m^2$ $d^{-1}$ of water-soluble Fe-EDTA) that were approximately 2 fold higher than the
347 Fe supply for maximal growth. However, *A. marina* (the dominant species affected by the
348 dieback at the study site) were unaffected by Fe at these concentrations. Fe concentrations
349 can be high in acid sulphate soils, but Johnston et al. (2016) observed no *A. marina* mortality
350 in Fe concentrations of 7-15 fold above normal. To our knowledge, no research has tested the
351 toxicity of Fe in *A. marina* at highly elevated concentrations of bioavailable $Fe^{2+}$.
352 Considering that other mangrove species are affected by Fe toxicity at twofold the optimal Fe
353 availability, it is quite possible that a 30-90 fold increase in Fe could be an additional stressor
354 to mangroves already stressed by low water availability.
355

https://doi.org/10.5194/bg-2019-478
Preprint. Discussion started: 16 January 2020




**Fe in sediments -** Sediment cores also had differences in down core Fe profiles between living and dead mangrove areas (Figure 5a and b). Normalized Fe concentrations were lower in the upper 1 m of sediments in the dead mangrove area compared to the living but were very similar in sediments deeper than 1 m (Figure 5a and b). Similar trends were also observed in CRS sediment core profiles, which have ~40 % lower $FeS_2$ concentrations in the dead mangroves in comparison to the living mangrove sediments (Figure 6). Although mangrove sediment conditions are highly heterogenous (Zhu et al. 2006, Zhu and Aller 2012), the sediment core results are consistent with the wood data. Both sediment and wood suggest a general trend of iron sulphide mineral oxidation, leading to increased Fe mobility in the dead mangrove area compared to the living area.

Sediment Fe losses due to variable periods of oxidation and reduction, as implied by Fe profiles (Figures 3, 4 & 6), would also suggest an outwelling of Fe to the ocean. We estimate Fe outwelling by comparing $FeS_2$ concentrations in living and dead mangrove sediment cores based on the assumptions that (1) all Fe was originally in the form of $FeS_2$ and (2) tree Fe uptake is a minor loss pathway. The losses of Fe from the dead mangrove sediment would be equivalent to 87±163 mmol $m^2$ $d^{-1}$. The replication of CRS sediment cores (n = 4) limits the accuracy of our estimates. However, these fluxes are remarkably similar to short-term porewater-derived dissolved Fe fluxes (79±75 mmol $m^2$ $d^{-1}$) estimated for a healthy temperate saltmarsh/mangrove system (Holloway et al. 2018), building confidence in our estimates.

If our sediment cores in dead and living mangroves are representative of changes within the entire dieback area (7400 ha), then total Fe losses from the dieback event could be equivalent to 87±163 Gg Fe. This loss is equivalent to 12 – 50% of global annual Fe inputs to the surface ocean from aerosols (Jickells et al. , Fung et al. 2000, Elrod et al. 2004). Since the surface ocean can be Fe limited, the consequences of Fe outwelling from this dieback event of such a magnitude could have an intense influence on ocean productivity.

**Wood density, growth trends and water use efficiency –** Trends in wood density also suggest differences in water availability between the living and dead mangrove areas. Clear decreases in normalised wood density were observed during the mangrove mortality event (Figure 8). Similar to trends in wood Fe, the wood density values in the living and dead forest areas were correlated to climatic indicators (Appendix 1). Unlike most trees, *A. marina* has decreased wood density with decreased growth rates due to a reduction in large xylem vessels (Santini et al., 2012). Therefor the observed decreases in wood density likely reflect lower growth rates, however the annual scale resolution of $^{14}C$ ages prevented detection of this short term change in growth rate. These clear decreases in wood density prior to tree mortality are therefore an indication of stress since decreased growth rates of mangroves can be associated with decreased water availability (Verheyden et al. 2005, Schmitz et al. 2006, Santini et al. 2013) which is also directly related to increased salinity. Low rainfall conditions and increased temperatures increase both evaporation and evapotranspiration while reducing freshwater inputs (Medina and Francisco 1997, Hoppe-Speer et al. 2013), partially explaining tree stress prior to the dieback.

Interestingly, no decrease in density was observed in the upper intertidal area of the dead mangroves (Figure 8), despite the clear increase in Fe during the dieback in this tree (Figure 3). This suggests that no change in growth occurred prior to tree mortality, implying rapid mortality in this case. The upper intertidal area of the dead mangroves may have been living at the limit of its tolerance range for water availability or salinity prior to the dieback, as suggested by extremely high groundwater salinities in the intertidal areas of dead and living

https://doi.org/10.5194/bg-2019-478
Preprint. Discussion started: 16 January 2020




mangrove forests eight months post dieback event (Figure 7c). No decrease in wood density was observed in the lower intertidal area of the living mangroves, which is consistent with both variation in concentration of Fe and tree growth rate data. Together, these data suggest that the lower intertidal area of the living mangroves was not exposed to the same conditions during the dieback event as areas in the dead mangroves higher in the intertidal zone (Figures 3, 8 & 9). These results suggest a gradient of water availability, from extremely low availability at the upper intertidal zone of the dead mangrove area to high/optimal availability at the lower intertidal zone of the living mangrove area. Since the elevation profiles are similar in the dead and living mangrove areas in the lower and mid intertidal areas (Figure 1), it is possible that the difference in Fe trends between the mangrove areas are associated with groundwater flows.

Mean growth rates of trees in living (4.4 ± 3.6 mm $yr^{-1}$) and dead (5.3 ± 3.5 mm $yr^{-1}$) mangrove areas are similar to rates measured by Santini et al., (2013) in *A. marina* in arid Western Australia (4.1 to 5.3 mm $yr^{-1}$). However, there was ~10 fold greater variability because samples were collected from the upper, mid and lower intertidal zone, while Santini et al. (2012) sampled from the lower intertidal zone only. De-trended growth rate data showed no consistent differences in growth trends were identified between mangrove areas (Figure 8). The lower intertidal sample of the living mangroves grew more quickly during the dieback, which may suggest optimal conditions during this time. This may be due to increased nutrient availability due to litterfall inputs of organic matter from nearby stressed trees. All other samples show no indication of reduced growth prior to or during the mortality event (Table 1). We suggest that climatic conditions drove very low growth rates during the dieback event, as indicated by wood density data (Figure 8) and previous studies that found low growth during droughts (Cook et al., 1977; Santini et al., 2013).

A significant difference in mean $\delta^{13}C$ and WUE between living or dead mangrove areas was observed in the upper intertidal zone (T-test, P = 0.02), but not in the mid or lower intertidal zones (Figure 7b). This is consistent with the zonation of mangrove mortality which occurred predominantly in the upper intertidal areas (Duke et al., 2017). The consistent decrease in WUE suggests that water availability has been increasing over time in all intertidal areas since the 1990's (Figure 7a). This is supported by generally increasing precipitation since 1980's (Figure 2), which enhanced mangrove areas in the Gulf of Carpentaria prior to this dieback event (Asbridge et al. 2016). Therefore, climatic conditions were initially favourable over the plants lifetime and trees may have been insufficiently acclimated to withstand drought and low soil water availability during the dieback. Overall, this highlights the important role of extreme climatic events counterbalancing mangrove responses to gradual climate trends (Harris et al. 2018).

**Limitations** - This study is inherently limited in its spatial extent. Thus, the differences in Fe between samples from living and dead mangrove areas may be due to factors other than mangrove mortality. However, the consistency of results from multiple methods and sample types gives confidence in the interpretation that recent changes in sediment geochemistry have occurred associated with extreme drought and low sea level events.

Our analysis benefited from the development of high precision $^{14}C$ dating of mangrove wood samples (with age uncertainties of 1-3 calendar years; see Table 1) that rely on atmospheric bomb $^{14}C$ content resulting from above-ground nuclear testing mostly in the late 1950's and early 1960's (Hua and Barbetti 2004a). The complexity in the wood development of *A.*

https://doi.org/10.5194/bg-2019-478
Preprint. Discussion started: 16 January 2020




*marina* creates uncertainties (Robert et al. 2011). *Avicennia marina* secondary growth is atypical, displaying consecutive bands of xylem and phloem which can result in multiple cambia (i.e. the tissue providing undifferentiated cells for the growth of plants) being simultaneously active (Schmitz et al., 2006; Robert et al., 2011). Furthermore, *A. marina* cambia display non-cylindrical or asymmetrical growth (Maxwell et al. 2018). These characteristics of *A. marina* atypical growth can influence our results as there is variation within each stem.

As younger wood grows on the exterior of the tree, errors associated with ages do not introduce uncertainty in the direction of trends but decrease the ability of finding correlated trends with climatic variables (Van Der Sleen et al. 2015). In spite of these uncertainties, the strong cross correlations displayed in Figure 4, with minimal time lag suggest that the dendrochronology results are robust, and that climate variability drives long-term Fe cycling in the coastal mangroves of the Gulf of Carpentaria.

**Summary and Conclusions**

Differences in sediment redox conditions during the dieback event were evident in all wood and sediment data from living and dead mangrove areas. Patterns in Fe concentrations in wood and sediment samples and climate, suggest that sediment oxidation occurred in combination with unprecedented low sea levels and low rainfall. As the elevation of dead and living mangrove areas was very similar, we suggest that the differences in tree survival between areas were probably due to higher groundwater availability in the living site. The increased oxygen permeation into sediments likely resulted in the oxidation of bioauthigenic pyrite, which transformed into aqueous and bioavailable $Fe^{2+}$. If further oxidation occured, $Fe^{2+}$ transforms into particulate Fe oxides. These Fe oxides are highly reactive and any subsequent short-term reduction (e.g. with tidal inundation) would also result in mobilization of Fe as $Fe^{2+}$. Evidence of plant Fe uptake and losses of Fe from sediments are consistent with this hypothesized Fe mobilization. The dieback event was likely a period of transitioning redox states in a heterogenous sediment matrix, which resulted in areas of mangrove sediments with low water availability combined with porewaters enriched in bioavailable Fe (Figure 9).

https://doi.org/10.5194/bg-2019-478
Preprint. Discussion started: 16 January 2020




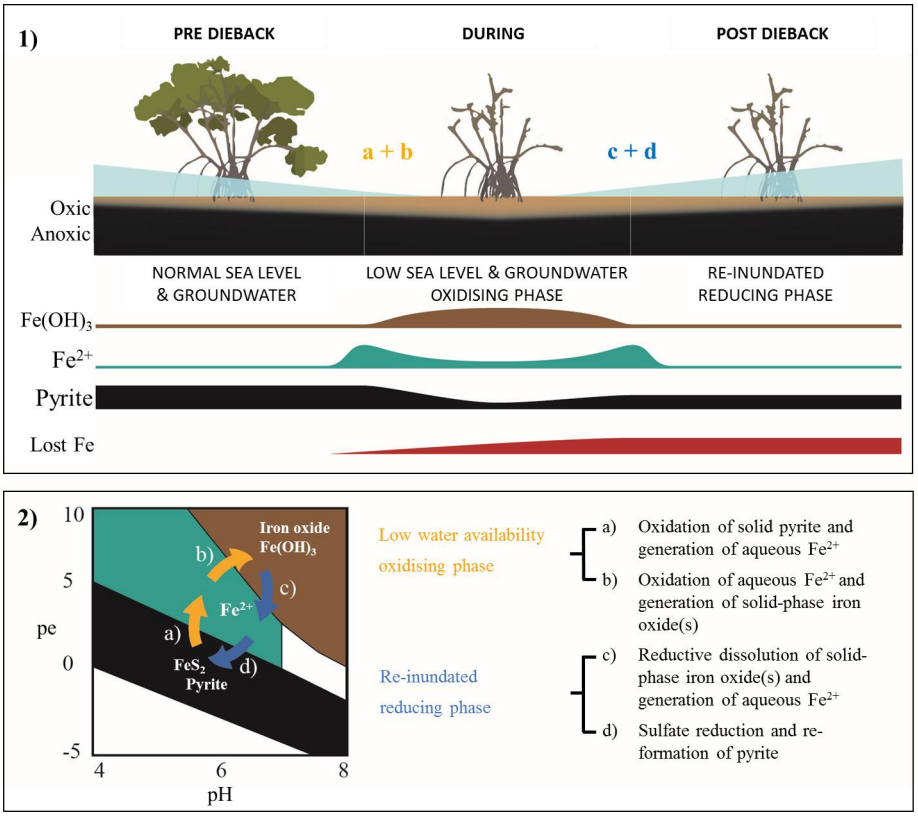


**Figure 9. Conceptual diagram of Fe speciation under different sediment redox, pH conditions and a) how speciation changes would be influenced by sea level and groundwater. Under increased redox conditions b) pyrite oxidation causes Fe transformation to bioavailable $Fe^{2+}$ and particulate $Fe(OH)_3$, consequent reduction of $Fe(OH)_3$**

Our data suggest that the climate-driven changes in sediment geochemistry resulted in extremely low water availability and drove the mangrove dieback. Mangrove dieback may also be associated with increased concentrations of bioavailable $Fe^{2+}$ in porewaters that occurred during this time of low water availability. Estimated losses of Fe from sediments were consistent with the observed plant uptake and suggest Fe mobilisation due to sediment oxidation (and subsequent reduction). This Fe mobilisation may also have led to significant Fe inputs to the ocean. This study supports climate observations suggesting that the Gulf of Carpentaria dieback was strongly driven by an extreme ENSO event (Harris et al. 2017). Climate change is increasing the intensity of ENSO events and climate extremes (Lee and McPhaden 2010, Cai et al. 2014, Freund et al. 2019) and increasing sea level variability (Widlansky et al. 2015), which is impacting on mangrove forests in arid coastlines (Lovelock et al. 2017). This study therefore revealed a geochemical mechanism that may also contribute to mangrove stress and dieback, building on the premise that the dieback event was associated with climate change (Harris et al. 2018). Further research is necessary to confirm the role of Fe in the mortality event, to constrain potential Fe losses to the ocean from sediments and to understand thresholds for Fe toxicities in *Avicennia marina*.

https://doi.org/10.5194/bg-2019-478
Preprint. Discussion started: 16 January 2020


Biogeosciences Discussions
Open Access
EGU

**Acknowledgements**

JZ Sippo acknowledges funding support and access to ANSTO facilities from AINSE which made this project possible. We would like to thank Jocelyn Turnbull for giving us permission to use atmospheric $^{14}C$ data extended to 2017 from Baring Head (Wellington). The study was funded by the Australian Research Council (DE150100581, DP180101285, DE160100443, DP150103286 and LE140100083).

https://doi.org/10.5194/bg-2019-478
Preprint. Discussion started: 16 January 2020




## References

Alber, M., E. M. Swenson, S. C. Adamowicz and I. A. Mendelssohn (2008). "Salt Marsh Dieback: An overview of recent events in the US." *Estuar. Coast. Shelf Sci.* **80**(1): 1-11.

Alongi, D. M. (2015). "The Impact of Climate Change on Mangrove Forests." *Current Climate Change Reports* **1**(1): 30-39.

Asbridge, E., R. Bartolo, C. M. Finlayson, R. M. Lucas, K. Rogers and C. D. Woodroffe (2019). "Assessing the distribution and drivers of mangrove dieback in Kakadu National Park, northern Australia." *Estuar. Coast. Shelf Sci.* **228**: 106353.

Asbridge, E., R. Lucas, C. Ticehurst and P. Bunting (2016). "Mangrove response to environmental change in Australia's Gulf of Carpentaria." *Ecology and evolution* **6**(11): 3523-3539.

Barbier, E. B., S. D. Hacker, C. Kennedy, E. W. Koch, A. C. Stier and B. R. Silliman (2011). "The value of estuarine and coastal ecosystem services." *Ecol. Monogr.* **81**(2): 169-193.

Brookhouse, M. (2006). "Eucalypt dendrochronology: past, present and potential." *Aust. J. Bot.* **54**(5): 435-449.

Burdige, D. J. (2011). "Estuarine and coastal sediments – coupled biogeochemical cycling." *Treatise on Estuarine and Coastal Science* **5**: 279-316.

Bureau of Meteorology (2019). "Climate data online." Retrieved 12/08/19, from http://www.bom.gov.au/climate/data/.

Burton, E. D., R. T. Bush and L. A. Sullivan (2006). "Sedimentary iron geochemistry in acidic waterways associated with coastal lowland acid sulfate soils." *Geochim. Cosmochim. Acta* **70**(22): 5455-5468.

Burton, E. D., L. A. Sullivan, R. T. Bush, S. G. Johnston and A. F. Keene (2008). "A simple and inexpensive chromium-reducible sulfur method for acid-sulfate soils." *Appl. Geochem.* **23**(9): 2759-2766.

Cai, W., S. Borlace, M. Lengaigne, P. van Rensch, M. Collins, G. Vecchi, A. Timmermann, A. Santoso, M. J. McPhaden, L. Wu, M. H. England, G. Wang, E. Guilyardi and F.-F. Jin (2014). "Increasing frequency of extreme El Niño events due to greenhouse warming." *Nature Climate Change* **4**: 111.

https://doi.org/10.5194/bg-2019-478
Preprint. Discussion started: 16 January 2020




550 Donato, D. C., J. B. Kauffman, D. Murdiyarso, S. Kurnianto, M. Stidham and M. Kanninen
551 (2011). "Mangroves among the most carbon-rich forests in the tropics." *Nature Geosci* **4**(5):
552 293-297.

553
554 Elrod, V. A., W. M. Berelson, K. H. Coale and K. S. Johnson (2004). "The flux of iron from
555 continental shelf sediments: A missing source for global budgets." *Geophys. Res. Lett.*
556 **31**(12).

557
558 Farquhar, G., K. Hubick, A. Condon and R. Richards (1989). Carbon isotope fractionation
559 and plant water-use efficiency. *Stable isotopes in ecological research*, Springer**:** 21-40.

560
561 Farquhar, G. and R. Richards (1984). "Isotopic composition of plant carbon correlates with
562 water-use efficiency of wheat genotypes." *Funct. Plant Biol.* **11**(6): 539-552.

563
564 Fink, D., M. Hotchkis, Q. Hua, G. Jacobsen, A. M. Smith, U. Zoppi, D. Child, C. Mifsud, H.
565 van der Gaast and A. Williams (2004). "The antares AMS facility at ANSTO." *Nuclear*
566 *Instruments and Methods in Physics Research Section B: Beam Interactions with Materials*
567 *and Atoms* **223**: 109-115.

568
569 Freund, M. B., B. J. Henley, D. J. Karoly, H. V. McGregor, N. J. Abram and D. Dommenget
570 (2019). "Higher frequency of Central Pacific El Niño events in recent decades relative to past
571 centuries." *Nature Geoscience* **12**(6): 450-455.

572
573 Fung, I. Y., S. K. Meyn, I. Tegen, S. C. Doney, J. G. John and J. K. Bishop (2000). "Iron
574 supply and demand in the upper ocean." *Global Biogeochem. Cycles* **14**(1): 281-295.

575
576 Google Earth (2019). "Karumba, Qld, Australia". Digital Globe

577
578 Gilman, E. L., J. Ellison, N. C. Duke and C. Field (2008). "Threats to mangroves from
579 climate change and adaptation options: A review." *Aquat. Bot.* **89**(2): 237-250.

580
581 Hamilton, S. E. and D. Casey (2016). "Creation of a high spatio-temporal resolution global
582 database of continuous mangrove forest cover for the 21st century (CGMFC-21)." *Global*
583 *Ecol. Biogeogr.* **25**(6): 729-738.

584
585 Harris, R. M. B., L. J. Beaumont, T. R. Vance, C. R. Tozer, T. A. Remenyi, S. E. Perkins-
586 Kirkpatrick, P. J. Mitchell, A. B. Nicotra, S. McGregor, N. R. Andrew, M. Letnic, M. R.
587 Kearney, T. Wernberg, L. B. Hutley, L. E. Chambers, M. S. Fletcher, M. R. Keatley, C. A.
588 Woodward, G. Williamson, N. C. Duke and D. M. J. S. Bowman (2018). "Biological
589 responses to the press and pulse of climate trends and extreme events." *Nature Climate*
590 *Change* **8**(7): 579-587.

591

https://doi.org/10.5194/bg-2019-478
Preprint. Discussion started: 16 January 2020




592 Harris, T., P. Hope, E. Oliver, R. Smalley, J. Arblaster, N. Holbrook, N. Duke, K. Pearce, K.
593 Braganza and N. Bindoff (2017). Climate drivers of the 2015 Gulf of Carpentaria mangrove
594 dieback. N. E. S. Program. Earth System and Climate Change Hub Technical Report 2,
595 Australian Government.

596
597 Hevia, A., R. Sánchez-Salguero, J. J. Camarero, A. Buras, G. Sangüesa-Barreda, J. D. Galván
598 and E. Gutiérrez (2018). "Towards a better understanding of long-term wood-chemistry
599 variations in old-growth forests: A case study on ancient Pinus uncinata trees from the
600 Pyrenees." *Sci. Total Environ.* **625**: 220-232.

601
602 Holloway, C. J., I. R. Santos and A. L. Rose (2018). "Porewater inputs drive Fe redox cycling
603 in the water column of a temperate mangrove wetland." *Estuar. Coast. Shelf Sci.* **207**: 259-
604 268.

605
606 Holloway, C. J., I. R. Santos, D. R. Tait, C. J. Sanders, A. L. Rose, B. Schnetger, H.-J.
607 Brumsack, P. A. Macklin, J. Z. Sippo and D. T. Maher (2016). "Manganese and iron release
608 from mangrove porewaters: a significant component of oceanic budgets?" *Mar. Chem.* **184**:
609 43-52.

610
611 Hoppe-Speer, S. C. L., J. B. Adams and A. Rajkaran (2013). "Response of mangroves to
612 drought and non-tidal conditions in St Lucia Estuary, South Africa." *Afr. J. Aquat. Sci.* **38**(2):
613 153-162.

614
615 Hua, Q. and M. Barbetti (2004a). "Review of tropospheric bomb 14C data for carbon cycle
616 modeling and age calibration purposes." *Radiocarbon* **46**(3): 1273-1298.

617
618 Hua, Q., M. Barbetti, U. Zoppi, D. Fink, M. Watanasak and G. E. Jacobsen (2004b).
619 "Radiocarbon in tropical tree rings during the Little Ice Age." *Nuclear Instruments and*
620 *Methods in Physics Research Section B: Beam Interactions with Materials and Atoms* **223**:
621 489-494.

622
623 Hua, Q., G. E. Jacobsen, U. Zoppi, E. M. Lawson, A. A. Williams, A. M. Smith and M. J.
624 McGann (2001). "Progress in radiocarbon target preparation at the ANTARES AMS Centre."
625 *Radiocarbon* **43**(2A): 275-282.

626
627 Jickells, T. and L. Spokes The biogeochemistry of iron in seawater, edited by: DR Turner,
628 KH, Wiley, Chichester, UK.

629
630 Johnston, S. G., A. F. Keene, R. T. Bush, E. D. Burton, L. A. Sullivan, L. Isaacson, A. E.
631 McElnea, C. R. Ahern, C. D. Smith and B. Powell (2011). "Iron geochemical zonation in a
632 tidally inundated acid sulfate soil wetland." *Chem. Geol.* **280**(3): 257-270.

633

https://doi.org/10.5194/bg-2019-478
Preprint. Discussion started: 16 January 2020




634 Johnston, S. G., B. Morgan and E. D. Burton (2016). "Legacy impacts of acid sulfate soil
635 runoff on mangrove sediments: Reactive iron accumulation, altered sulfur cycling and trace
636 metal enrichment." *Chem. Geol.* **427**: 43-53.

637
638 Jones, D. A., W. Wang and R. Fawcett (2009). "High-quality spatial climate data-sets for
639 Australia." *Australian Meteorological and Oceanographic Journal* **58**(4): 233.

640
641 Keene, A. F., S. G. Johnston, R. T. Bush, E. D. Burton, L. A. Sullivan, M. Dundon, A. E.
642 McElnea, C. D. Smith, C. R. Ahern and B. Powell (2014). "Enrichment and heterogeneity of
643 trace elements at the redox-interface of Fe-rich intertidal sediments." *Chem. Geol.* **383**: 1-12.

644
645 Lee, T. and M. J. McPhaden (2010). "Increasing intensity of El Niño in the central-equatorial
646 Pacific." *Geophys. Res. Lett.* **37**(14).

647
648 Lovelock, C. E., D. R. Cahoon, D. A. Friess, G. R. Guntenspergen, K. W. Krauss, R. Reef, K.
649 Rogers, M. L. Saunders, F. Sidik and A. Swales (2015). "The vulnerability of Indo-Pacific
650 mangrove forests to sea-level rise." *Nature*.

651
652 Lovelock, C. E., I. C. Feller, R. Reef, S. Hickey and M. C. Ball (2017). "Mangrove dieback
653 during fluctuating sea levels." *Scientific Reports* **7**(1): 1680.

654
655 Maxwell, J. T., G. L. Harley and A. F. Rahman (2018). "Annual Growth Rings in Two
656 Mangrove Species from the Sundarbans, Bangladesh Demonstrate Linkages to Sea-Level
657 Rise and Broad-Scale Ocean-Atmosphere Variability." *Wetlands* **38**(6): 1159-1170.

658
659 McKee, K. L., I. A. Mendelssohn and M. D. Materne (2004). "Acute salt marsh dieback in
660 the Mississippi River deltaic plain: a drought-induced phenomenon?" *Global Ecol. Biogeogr.*
661 **13**(1): 65-73.

662
663 Medina, E. and M. Francisco (1997). "Osmolality and δ 13 C of leaf tissues of mangrove
664 species from environments of contrasting rainfall and salinity." *Estuar. Coast. Shelf Sci.*
665 **45**(3): 337-344.

666
667 Nguyen, H. T., P. Meir, L. Sack, J. R. Evans, R. S. Oliveira and M. C. Ball (2017). "Leaf
668 water storage increases with salinity and aridity in the mangrove Avicennia marina:
669 integration of leaf structure, osmotic adjustment and access to multiple water sources." *Plant,*
670 *Cell Environ.* **40**(8): 1576-1591.

671
672 Ogburn, M. B. and M. Alber (2006). "An investigation of salt marsh dieback in Georgia
673 using field transplants." *Estuaries and Coasts* **29**(1): 54-62.

674
675 Queensland Government (2019). "QldGlobe." Sourced from
676 https://qldglobe.information.qld.gov.au.

https://doi.org/10.5194/bg-2019-478
Preprint. Discussion started: 16 January 2020




677

678 Richards, D. R. and D. A. Friess (2016). "Rates and drivers of mangrove deforestation in
679 Southeast Asia, 2000–2012." *Proceedings of the National Academy of Sciences* **113**(2): 344-
680 349.

681

682 Robert, E. M., N. Schmitz, J. A. Okello, I. Boeren, H. Beeckman and N. Koedam (2011).
683 "Mangrove growth rings: fact or fiction?" *Trees* **25**(1): 49-58.

684

685 Santini, N. S., Q. Hua, N. Schmitz and C. E. Lovelock (2013). "Radiocarbon dating and wood
686 density chronologies of mangrove trees in arid Western Australia." *PloS one* **8**(11): e80116.

687

688 Santini, N. S., N. Schmitz and C. E. Lovelock (2012). "Variation in wood density and
689 anatomy in a widespread mangrove species." *Trees* **26**(5): 1555-1563.

690

691 Schmitz, N., A. Verheyden, H. Beeckman, J. G. KAIRO and N. Koedam (2006). "Influence
692 of a salinity gradient on the vessel characters of the mangrove species Rhizophora
693 mucronata." *Ann. Bot.* **98**(6): 1321-1330.

694

695 Silliman, B. R., J. Van De Koppel, M. D. Bertness, L. E. Stanton and I. A. Mendelssohn
696 (2005). "Drought, snails, and large-scale die-off of southern US salt marshes." *Science*
697 **310**(5755): 1803-1806.

698

699 Sippo, J. Z., C. E. Lovelock, I. R. Santos, C. J. Sanders and D. T. Maher (2018). "Mangrove
700 mortality in a changing climate: An overview." *Estuar. Coast. Shelf Sci.* **215**: 241-249.

701

702 Van Breemen, N. (1988). Redox Processes of Iron and Sulfur Involved in the Formation of
703 Acid Sulfate Soils. *Iron in Soils and Clay Minerals*. J. W. Stucki, B. A. Goodman and U.
704 Schwertmann. Dordrecht, Springer Netherlands**:** 825-841.

705

706 Van Der Sleen, P., P. Groenendijk, M. Vlam, N. P. Anten, A. Boom, F. Bongers, T. L. Pons,
707 G. Terburg and P. A. Zuidema (2015). "No growth stimulation of tropical trees by 150 years
708 of CO 2 fertilization but water-use efficiency increased." *Nature geoscience* **8**(1): 24.

709

710 Verheyden, A., F. De Ridder, N. Schmitz, H. Beeckman and N. Koedam (2005). "High-
711 resolution time series of vessel density in Kenyan mangrove trees reveal a link with climate."
712 *New Phytol.* **167**(2): 425-435.

713

714 Widlansky, M. J., A. Timmermann and W. Cai (2015). "Future extreme sea level seesaws in
715 the tropical Pacific." *Science Advances* **1**(8): e1500560.

716

717 Zhu, Q. and R. C. Aller (2012). "Two-dimensional dissolved ferrous iron distributions in
718 marine sediments as revealed by a novel planar optical sensor." *Mar. Chem.* **136**: 14-23.

719

https://doi.org/10.5194/bg-2019-478
Preprint. Discussion started: 16 January 2020




720 Zhu, Q., R. C. Aller and Y. Fan (2006). "Two-dimensional pH distributions and dynamics in
721 bioturbated marine sediments." *Geochim. Cosmochim. Acta* **70**(19): 4933-4949.

722

723

724

https://doi.org/10.5194/bg-2019-478
Preprint. Discussion started: 16 January 2020


Biogeosciences
Discussions
Open Access
EGU

725 **Appendix 1. Cross correlation function (CCF) analysis of the relationship between wood density and**
726 **climate data over time at one month resolution over a 12 month period prior and post dieback. Wood**
727 **samples are from the upper, mid and lower intertidal zones of the dead (red) and living (green) mangrove**
728 **areas. Blue horizontal dashed lines indicate P< 0.01 with n=125. Grey dashed vertical lines at zero lag**
729 **indicate dieback period.**
730

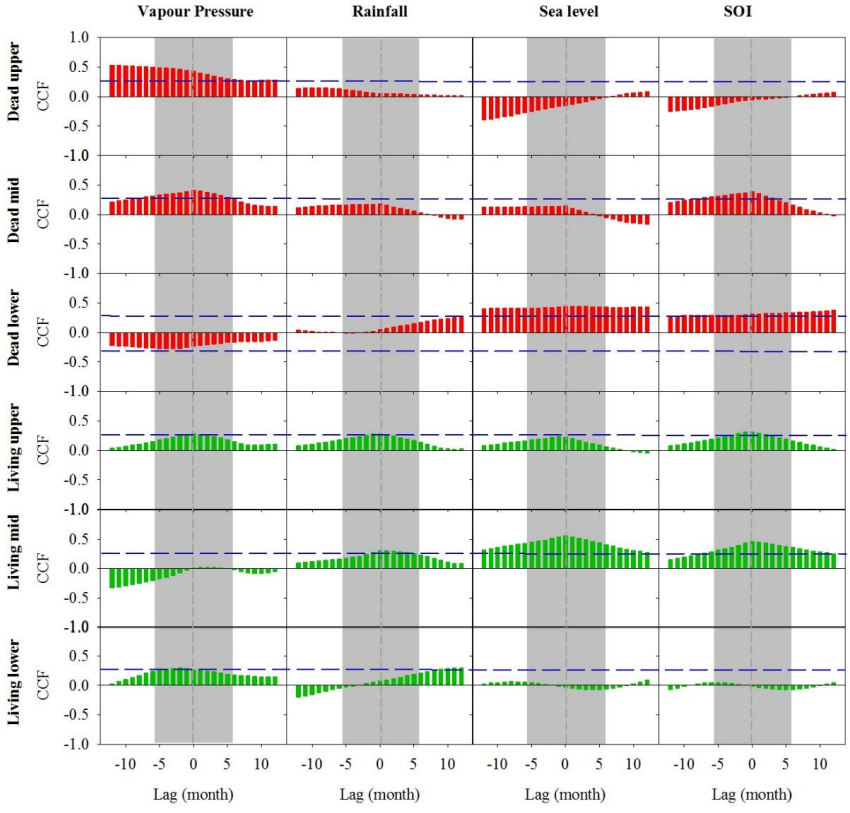


731
732